First DAS observations from the GeoLab fibre in Madeira, Portugal

Afonso Loureiro * [1,2], **David Schlaphorst** [2], **Luís Matias** [2], **Andreia Pereira** [2], **Carlos Corela** [2], **Susana Gonçalves** [2], **Rui Caldeira** [1]

[1]Agência Regional para o Desenvolvimento da Investigação, Tecnologia e Inovação, Funchal, Portugal, [2]IDL - Instituto Dom Luiz, Faculdade de Ciências, Universidade de Lisboa, 1749-016 Lisboa, Portugal

Author contributions: *Conceptualization*: Afonso Loureiro. *Software*: Afonso Loureiro, David Schlaphorst, Susana Gonçalves. *Formal Analysis*: Afonso Loureiro, David Schlaphorst, Andreia Pereira, Luís Matias, Carlos Corela. *Writing - Original draft*: Afonso Loureiro. *Writing - Review & Editing*: Afonso Loureiro, David Schlaphorst, Andreia Pereira, Susana Gonçalves. *Funding acquisition*: Luís Matias, Rui Caldeira.

S1 Supplemental material

Table S1 Teleseismic events M>5 recorded by global networks during the Distributed Acoustic Sensing data acquisition.

Time	Location			Distance	Magnitude	Description
	Latitude	Longitude	Depth			
2023-10-26T16:05:11	56.05° N	164.75° E	2 km	91.5°	M5.9	Komandorskiye Ostrova Region
2023-10-26T19:00:26	7.3° S	27.93° E	15 km	58.2°	M5.4	Democratic Republic of Congo
2023-10-27T03:02:24	17.58° S	173.77° W	35 km	154.5°	M5.6	Tonga Islands
2023-10-28T04:33:30	20.12°S	176.39° E	215 km	164.7°	M5.5	Fiji Islands Region
2023-10-28T05:31:58	10.22° S	161.30° W	69 km	140.5°	M5.5	Solomon Islands
2023-10-28T09:55:28	13.11° S	167.06° E	2 km	160.4°	M5.6	Vanuatu Islands
2023-10-29T04:32:08	19.42° S	168.76° E	80 km	166.1°	M6.0	Vanuatu Islands
2023-10-29T13:57:41	43.94° N	28.38° W	10 km	14.7°	M5.1	Northern Mid-Atlantic Ridge
2023-10-30T15:57:21	18.08° N	76.58° W	1 km	55.2°	M5.4	Jamaica Region
2023-10-31T11:10:56	17.62° S	179.03° W	552 km	158.2°	M6.5	Fiji Islands Region
2023-10-31T12:33:44	28.75° S	71.57° W	41 km	80.3°	M6.7	Near Coast of Central Chile (Figure 10)
2023-11-01T10:15:43	15.52° S	177.52° W	410 km	155.7°	M5.1	Fiji Islands Region
2023-11-01T12:51:15	10.93° N	93.06° E	94 km	100.4°	M5.1	Andaman Islands India Region
2023-11-01T21:04:45	10.06° S	123.75° E	51 km	137.4°	M6.1	Timor Region
2023-11-02T07:09:41	10.26° N	40.94° W	10 km	31.4°	M5.1	Northern Mid-Atlantic Ridge

*Corresponding author: maloureiro@fc.ul.pt

Table S2 Local and regional seismic events M>2 recorded by IPMA and EMSC networks during the Distributed Acoustic Sensing data acquisition.

Time	Location			Distance	Magnitude	Description
	Latitude	Longitude	Depth			
2023-10-27T14:21:01	32.43° N	16.27° W	4 km	49.9 km	M2.7	Desertas Islands (Figure 7)
2023-10-29T00:25:34	34.35° N	16.43° W	10 km	219.5 km	M2.4	North of Madeira
2023-10-29T10:02:32	27.62° N	15.41° W	20.6 km	548.1 km	Ml2.0	Canary Islands
2023-10-29T20:20:03	28.11° N	17.15° W	12.9 km	478.2 km	Ml2.3	Canary Islands
2023-10-29T21:51:53	28.04° N	17.15° W	16.3 km	486.00 km	Ml2.3	Canary Islands
2023-10-30T02:58:39	28.03° N	17.13° W	16.7 km	487.00 km	Ml2.8	Canary Islands
2023-10-30T09:32:41	28.01° N	17.11° W	8.1 km	489.1 km	Ml2.5	Canary Islands
2023-11-01T05:15:45	29.38° N	17.86° W	0.0 km	350.7 km	Ml2.0	Canary Islands
2023-11-01T09:10:44	27.67° N	18.26° W	40.6 km	544.4 km	Ml2.1	Canary Islands
2023-11-01T16:53:15	28.05° N	17.15° W	12.2 km	484.9 km	Ml2.1	Canary Islands
2023-11-01T20:04:28	27.96° N	15.16° W	8.6 km	518.2 km	Ml3.0	Canary Islands
2023-11-01T23:40:03	28.07° N	17.12° W	16.2 km	482.5 km	Ml2.7	Canary Islands
2023-11-02T04:10:12	28.57° N	17.89° W	6.0 km	438.5 km	Ml2.1	Canary Islands
2023-11-02T13:44:44	28.10° N	16.08° W	10.3 km	483.1 km	Ml2.0	Canary Islands

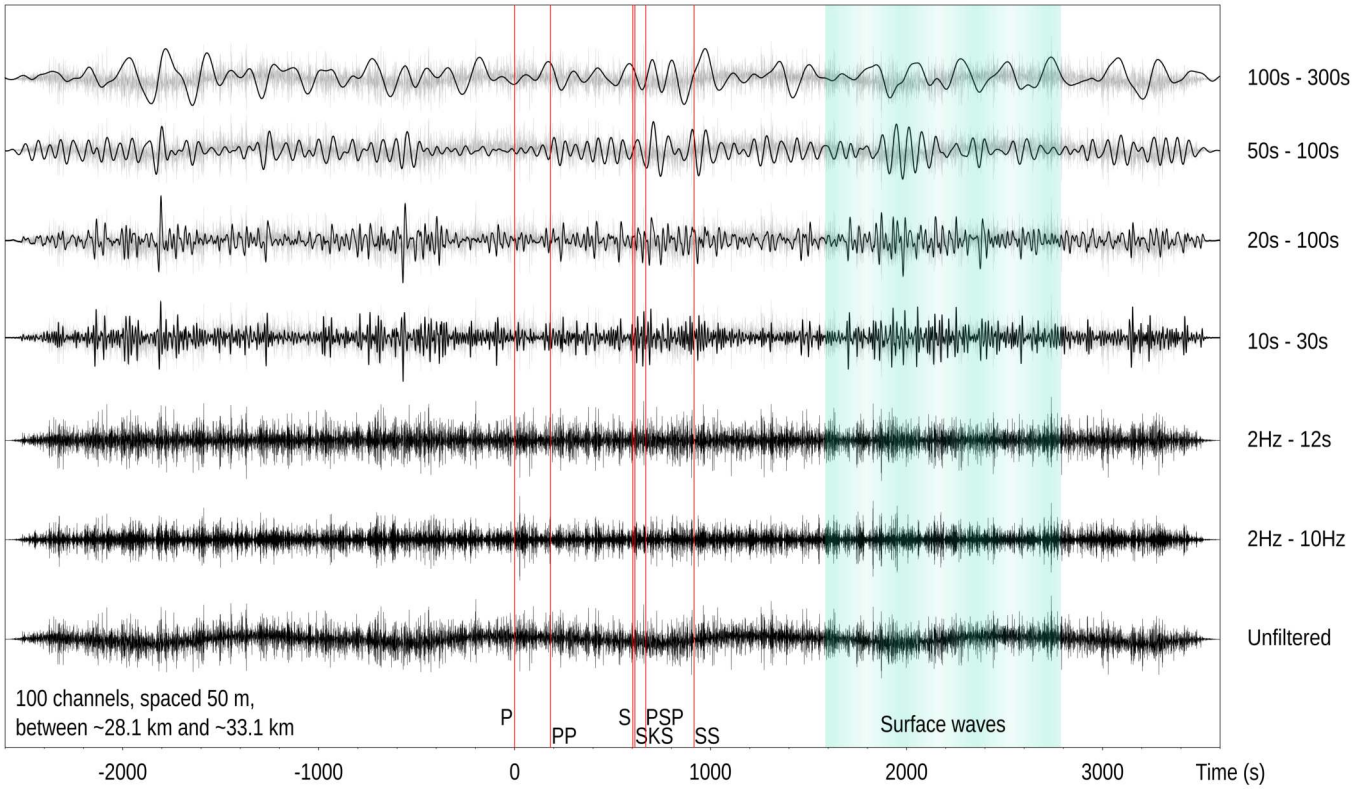

Figure S1 Broadband response for a teleseismic event. Different bandpass two-corner, zero-phase filters applied to a stack of 100 channels at each ∼50 m, between ∼28.1 km and ∼33.1 km, for a 6200 s window starting 2600 s before the predicted arrival of the P wave for the M_w 6.7 of 2023/10/31 12:33:44Z (see Figure 10). The top four traces (black lines) are overlaid on the unfiltered stacked data (grey lines). Red lines indicate predicted arrivals using TauP (Crotwell et al., 1999) with the iasp91 model (Kennett and Engdahl, 1991) for the coordinates of the first channel of the stack, corrected for the estimated time offset of the interrogator (see Section 2.1). The green band indicates surface wave arrivals.

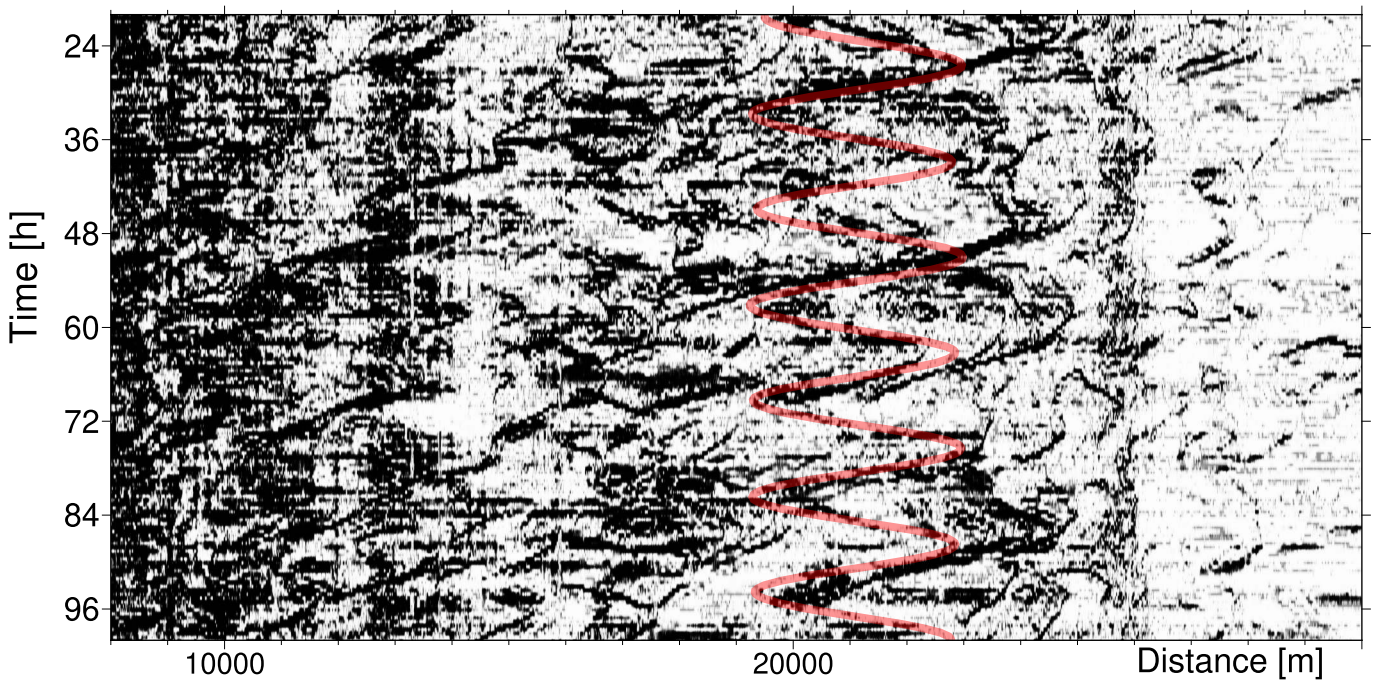

Figure S2 Enhanced contrast image of internal tides. Zoom on the region defined by the dashed rectangle in Figure 11, highlighting internal tides on the island slope. The semi-diurnal pattern can be tracked for more than 15 km. Red line shows tide heights modelled for Funchal, using the same scale as Figure 11c.

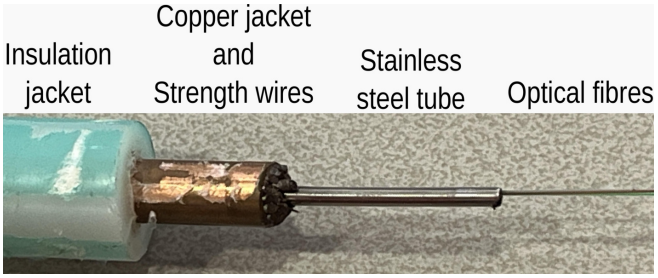

Figure S3 Photograph of a section of the GeoLab cable, with major structural parts identified. Not shown: armouring and outer jacket.

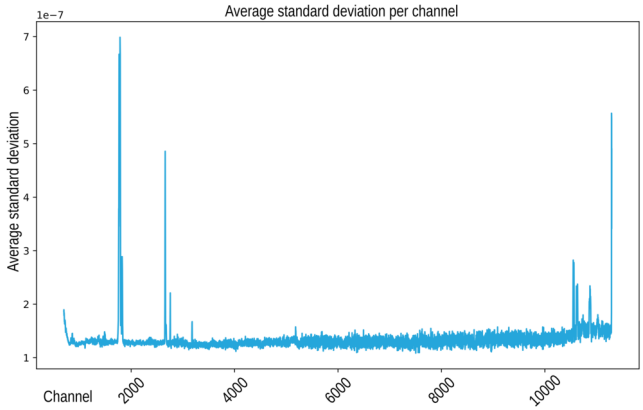

Figure S4 Average standard deviation on five minute windows for each channel from 2023/10/26 09:45:00Z to 2023/11/03 09:35:00Z. Sections of the cable that are presumed to be hanging and those where ringing is found have higher average standard deviation values (see Sections 2.2, 2.2.2). The step close to the end of the fibre is most likely linked to noise introduced by the reflection of the outgoing laser pulse at the end of the fibre, as discussed at the end of Section 2.2.

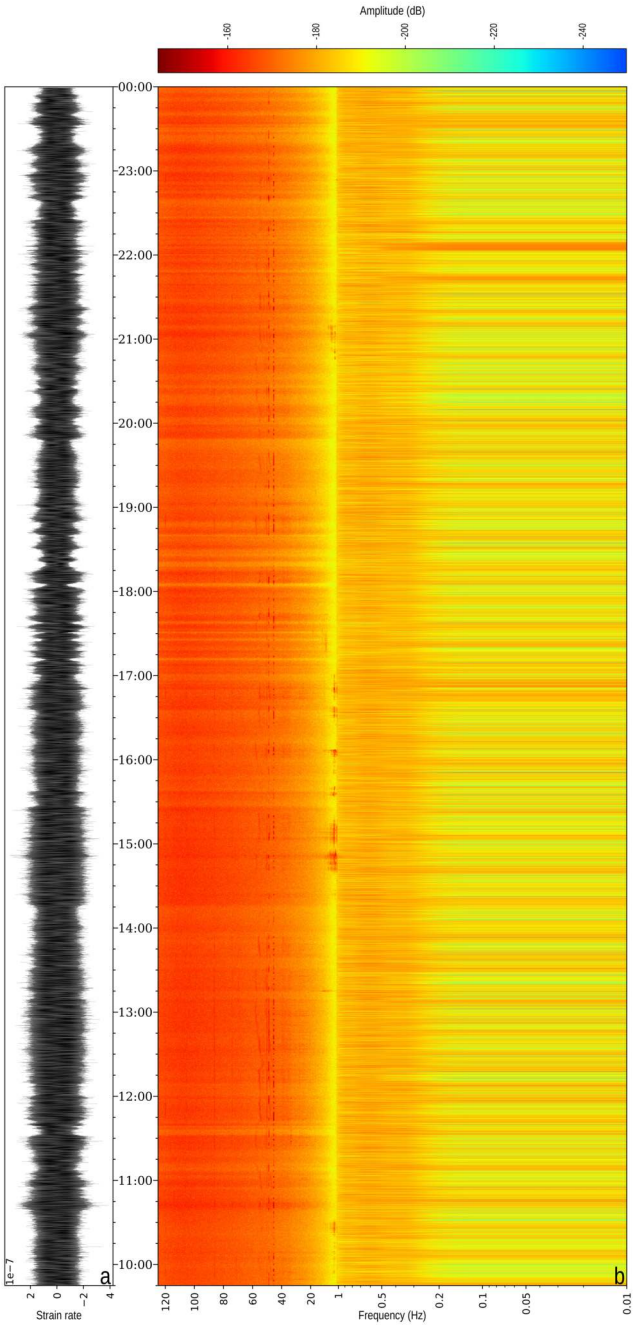

Figure S5 Spectrogram for 2023/10/26. a) Phase rate. b) Spectrogram from 100 s to 125 Hz for ∼14 h of data from a single channel at ∼16.3 km. Linear/logarithmic scale for frequencies above/below 1 Hz. $NFFT = 256$, overlap 50 %. Between 1 Hz and 5 Hz, harmonics from cable oscillation events are visible. At ∼45 Hz, anthropogenic noise is noticeable throughout the entire time. A possible small earthquake is apparent at 13:15:00.

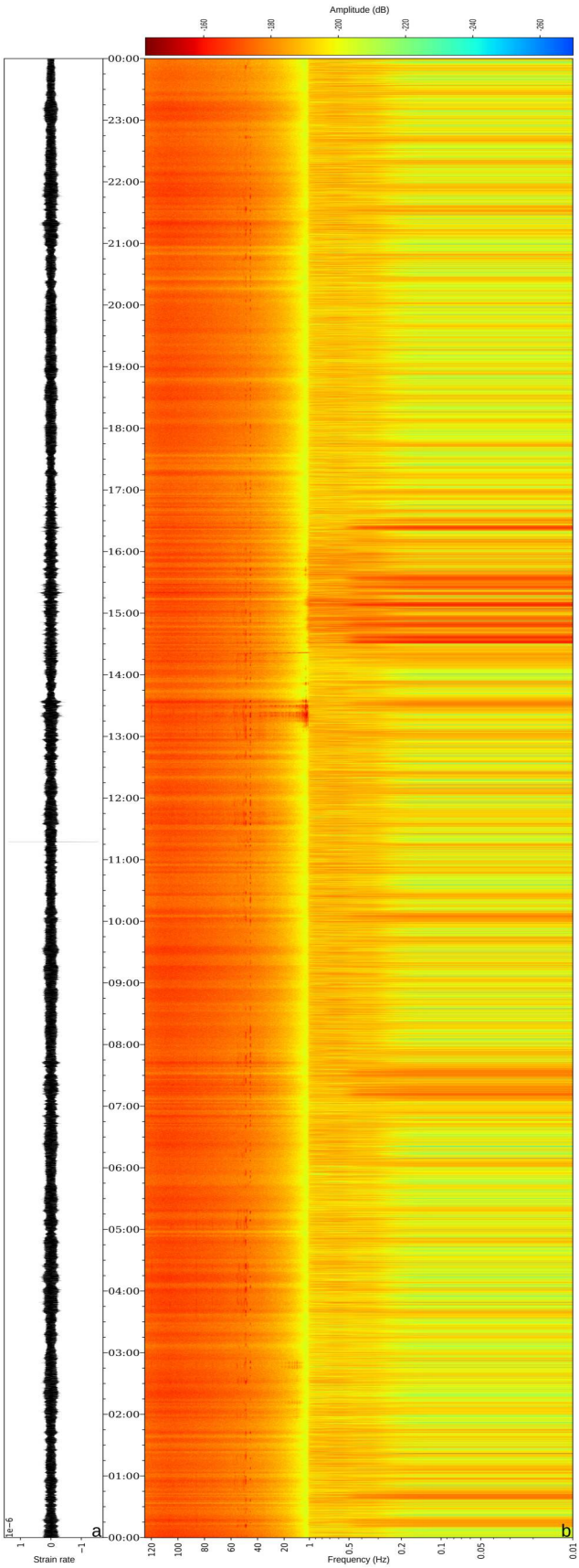

Figure S6 Spectrogram for 2023/10/27. a) Phase rate. b) Spectrogram from 100 s to 125 Hz for 24 h of data from a single channel at ∼21.5 km. Linear/logarithmic scale for frequencies above/below 1 Hz. $NFFT = 256$, overlap 50 %. Between 1 Hz and 5 Hz, harmonics from cable oscillation events are visible. At ∼45 Hz, anthropogenic noise is noticeable throughout the entire time. Semi-diurnal tidal patterns are discernible in the lower frequencies.

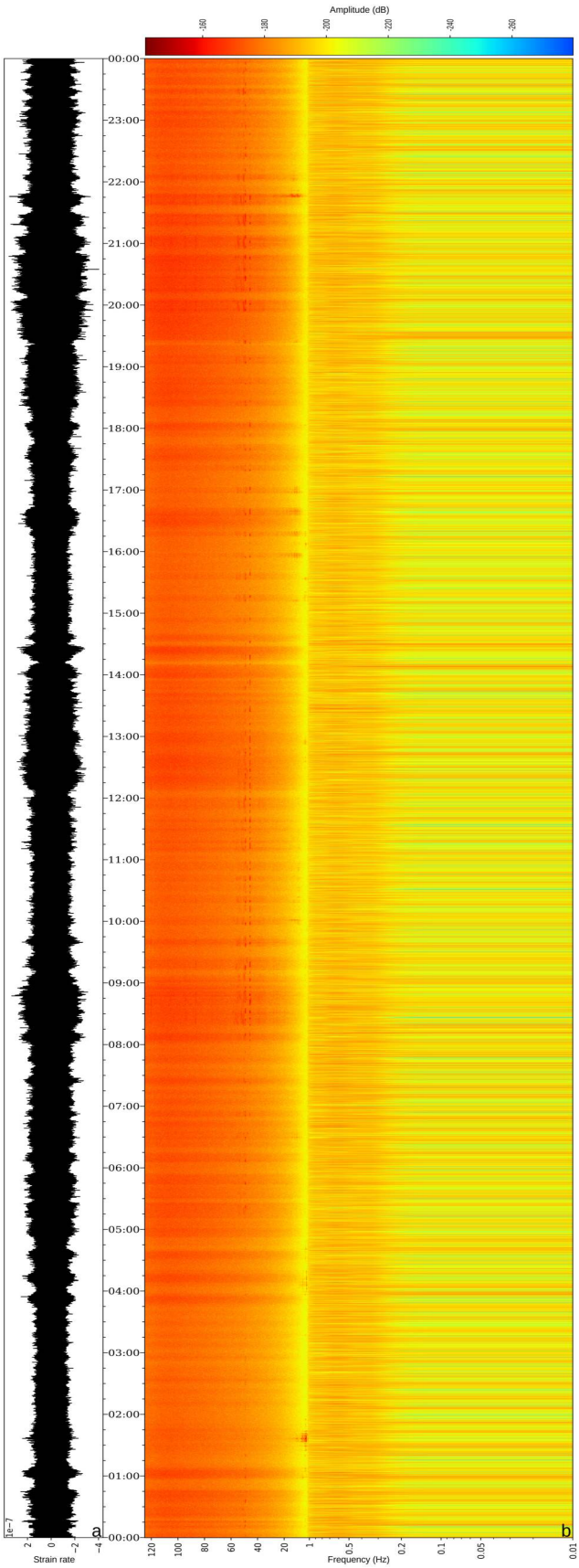

Figure S7 Spectrogram for 2023/10/28. a) Phase rate. b) Spectrogram from 100 s to 125 Hz for 24 h of data from a single channel at ∼36.7 km. Linear/logarithmic scale for frequencies above/below 1 Hz. $NFFT = 256$, overlap 50 %. Between 1 Hz and 5 Hz, harmonics from cable oscillation events are visible. At ∼45 Hz, anthropogenic noise is noticeable throughout the entire time. On the high frequencies, banding effects are apparent for most of the day.

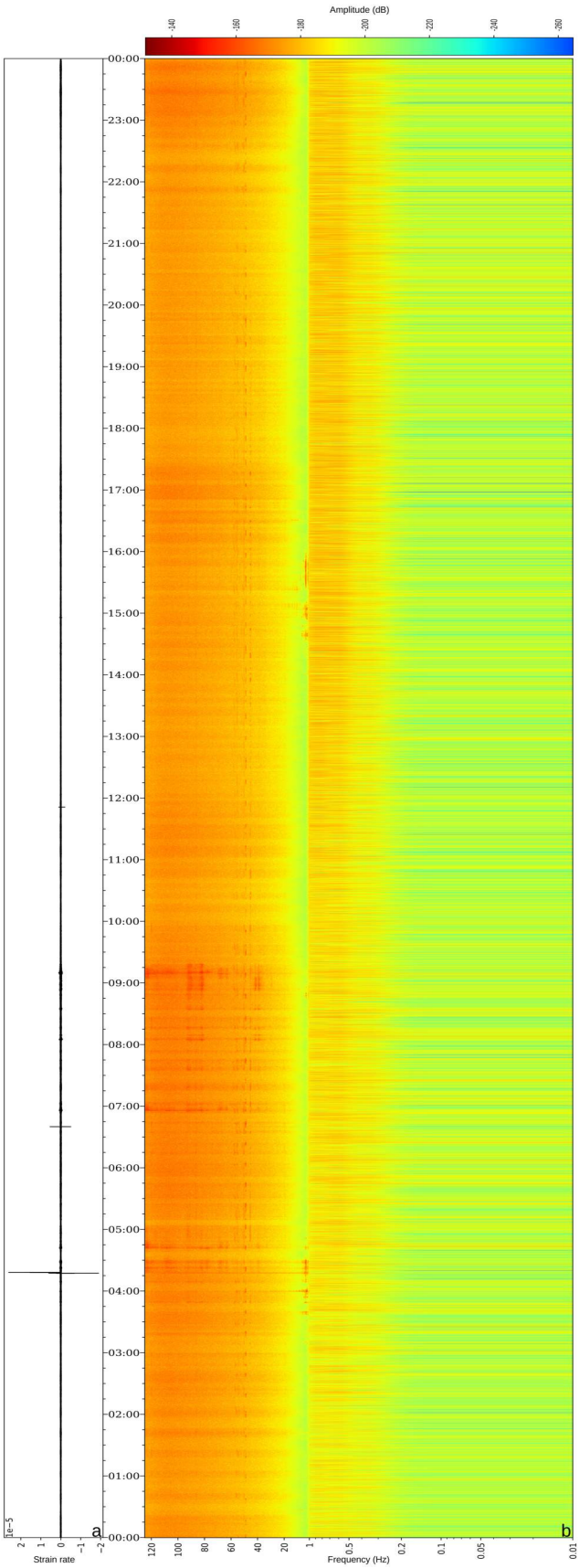

Figure S8 Spectrogram for 2023/10/29. a) Phase rate. b) Spectrogram from 100 s to 125 Hz for 24 h of data from a single channel at ∼52.1 km. Linear/logarithmic scale for frequencies above/below 1 Hz. $NFFT = 256$, overlap 50 %. Between 1 Hz and 5 Hz, harmonics from cable oscillation events are visible. At ∼45 Hz, anthropogenic noise is noticeable throughout the entire time.

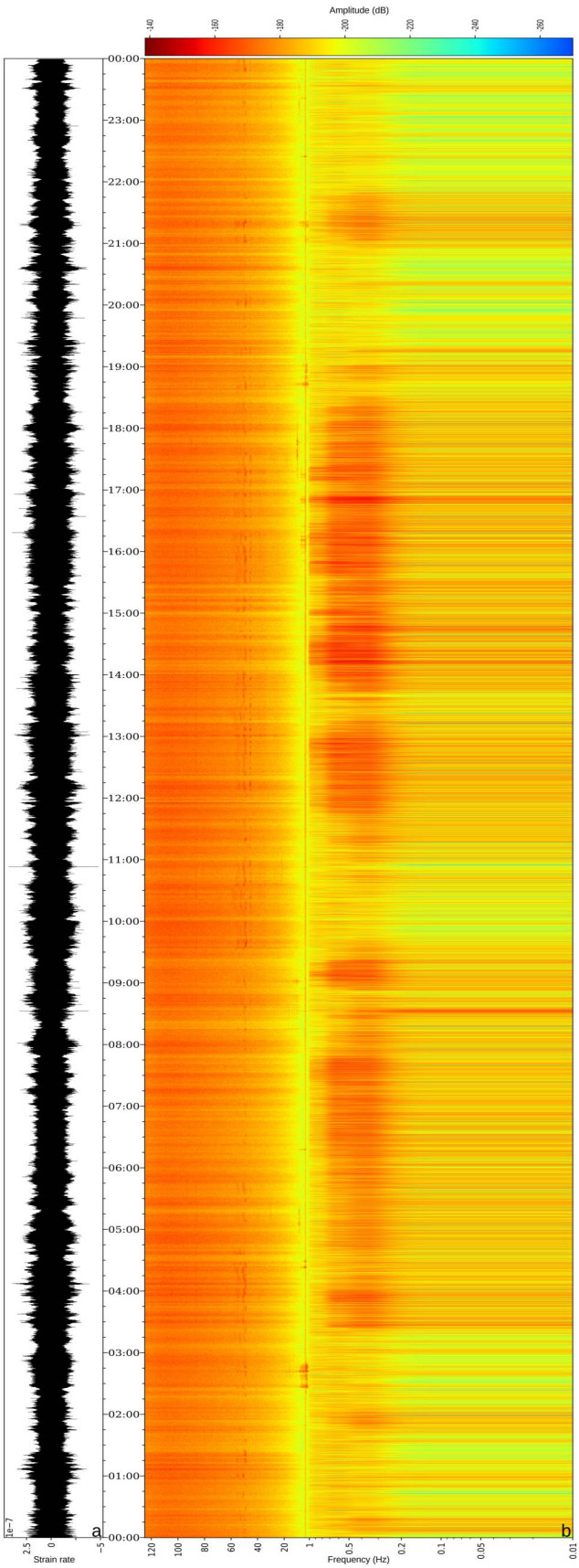

Figure S9 Spectrogram for 2023/10/30. a) Phase rate. b) Spectrogram from 100 s to 125 Hz for 24 h of data from a single channel at ∼26.6 km. Linear/logarithmic scale for frequencies above/below 1 Hz. $NFFT = 256$, overlap 50 %. Between 1 Hz and 5 Hz, harmonics from cable oscillation events are visible. At ∼45 Hz, anthropogenic noise is noticeable throughout the entire time. Semi-diurnal tidal patterns are discernible in the lower frequencies.

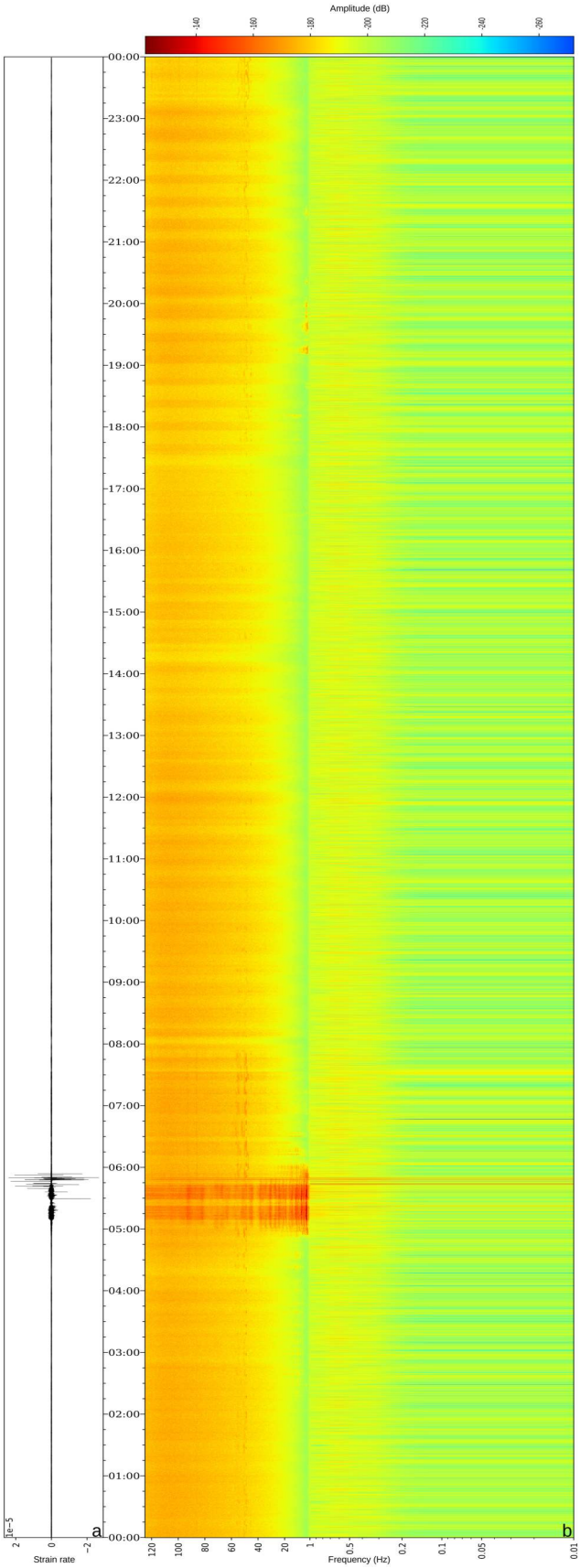

Figure S10 Spectrogram for 2023/10/31. a) Phase rate. b) Spectrogram from 100 s to 125 Hz for 24 h of data from a single channel at ∼36.8 km. Linear/logarithmic scale for frequencies above/below 1 Hz. $NFFT = 256$, overlap 50 %. Extreme amplitude harmonics from cable oscillation are visible, overpowering the spectrogram.

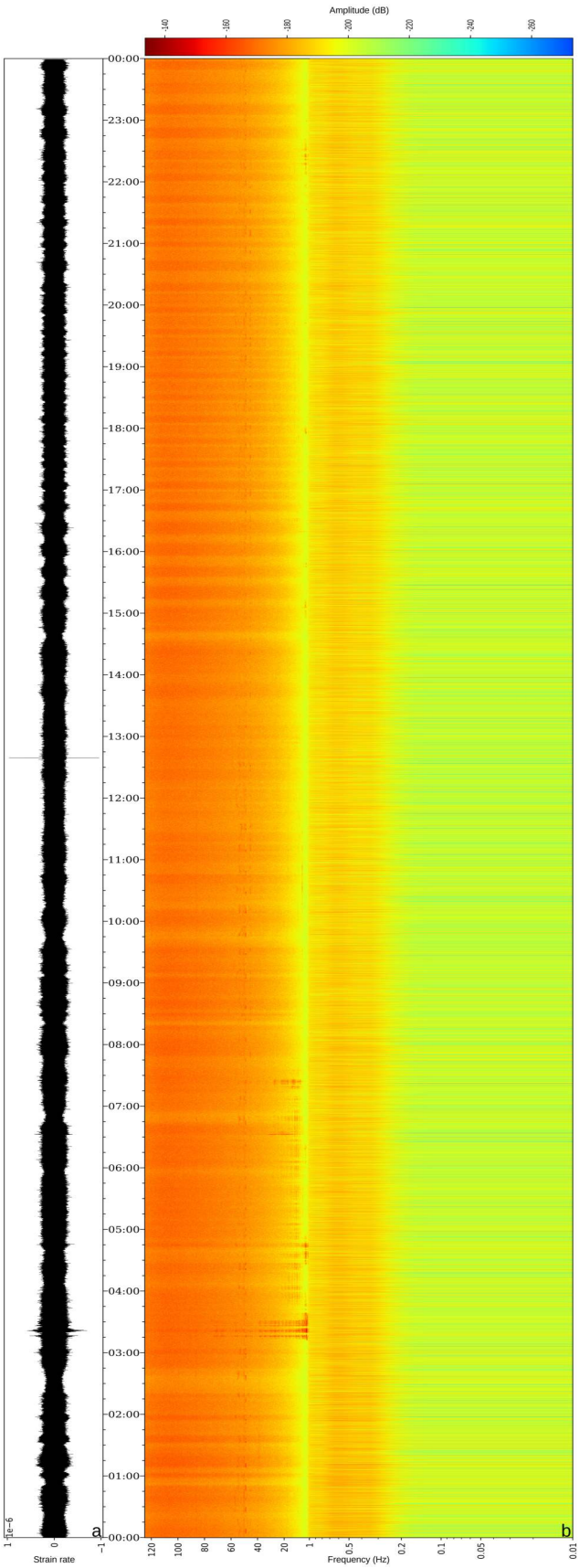

Figure S11 Spectrogram for 2023/11/01. a) Phase rate. b) Spectrogram from 100 s to 125 Hz for 24 h of data from a single channel at ∼57.2 km. Linear/logarithmic scale for frequencies above/below 1 Hz. $NFFT = 256$, overlap 50 %. Between 1 Hz and 5 Hz, harmonics from cable oscillation events are visible. At 03:30:00, the harmonics extend to above 40 Hz. At ∼45 Hz, anthropogenic noise is noticeable throughout the entire time.

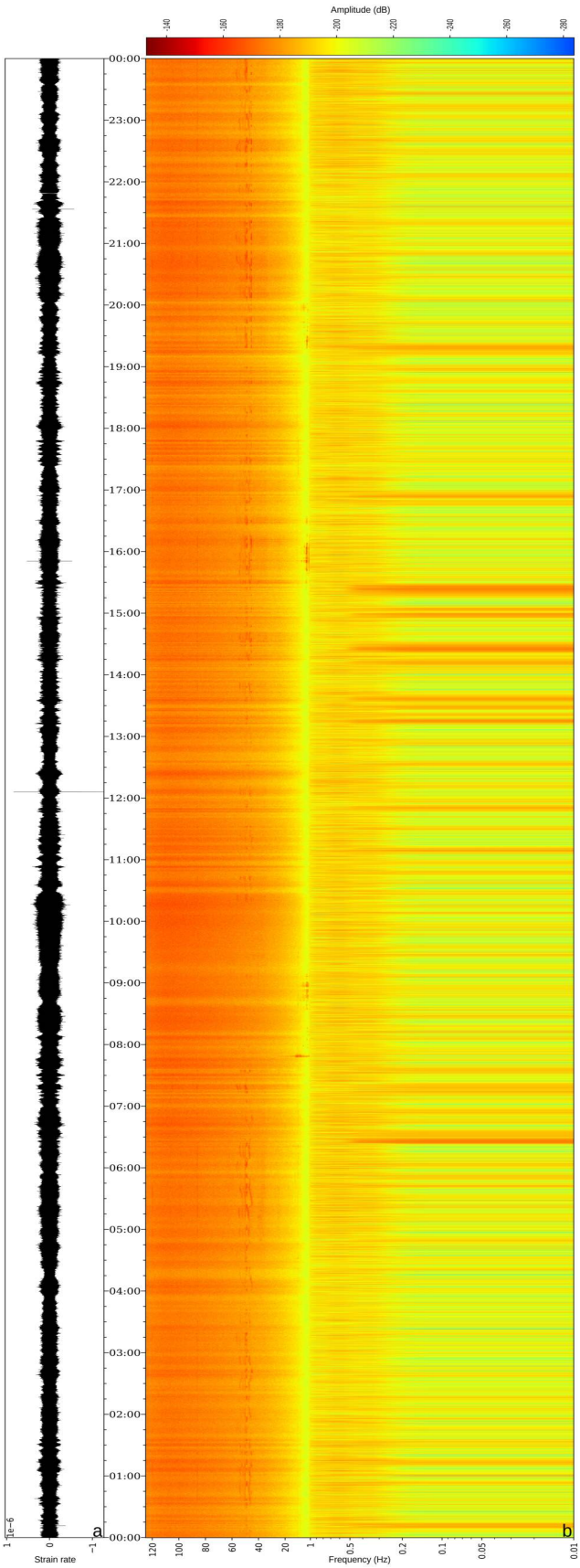

Figure S12 Spectrogram for 2023/11/02. a) Phase rate. b) Spectrogram from 100 s to 125 Hz for 24 h of data from a single channel at ∼16.4 km. Linear/logarithmic scale for frequencies above/below 1 Hz. $NFFT = 256$, overlap 50 %. Between 1 Hz and 5 Hz, harmonics from cable oscillation events are visible. At ∼45 Hz, anthropogenic noise is noticeable throughout the entire time. Semi-diurnal tidal patterns are discernible in the lower frequencies.

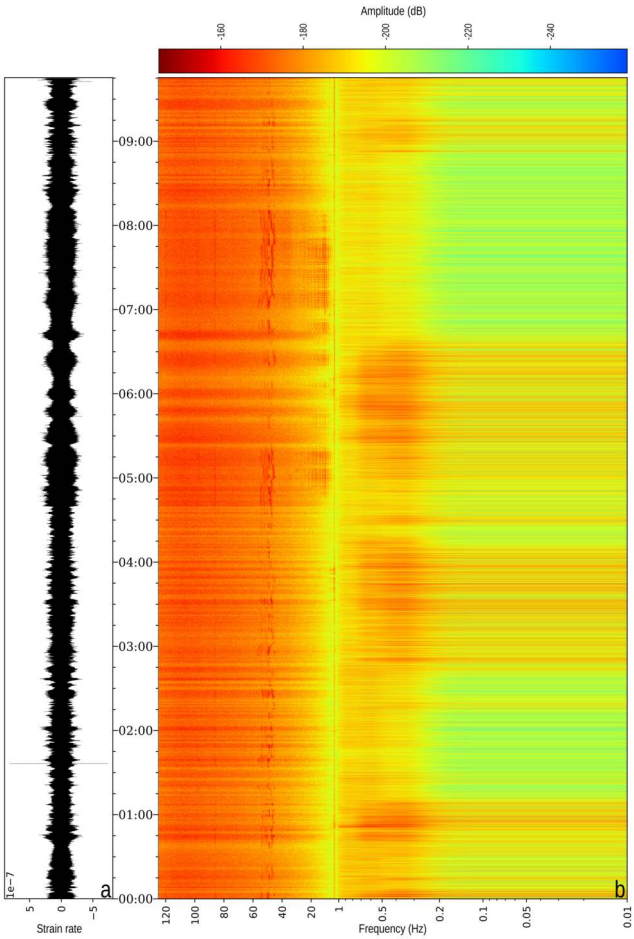

Figure S13 Spectrogram for 2023/11/23. a) Phase rate. b) Spectrogram from 100 s to 125 Hz for ∼10 h of data from a single channel at ∼26.5 km. Linear/logarithmic scale for frequencies above/below 1 Hz. $NFFT = 256$, overlap 50 %. Between 1 Hz and 20 Hz, harmonics from cable oscillation events are visible. At ∼45 Hz, anthropogenic noise is noticeable throughout the entire time. Semi-diurnal tidal patterns are discernible in the lower frequencies.

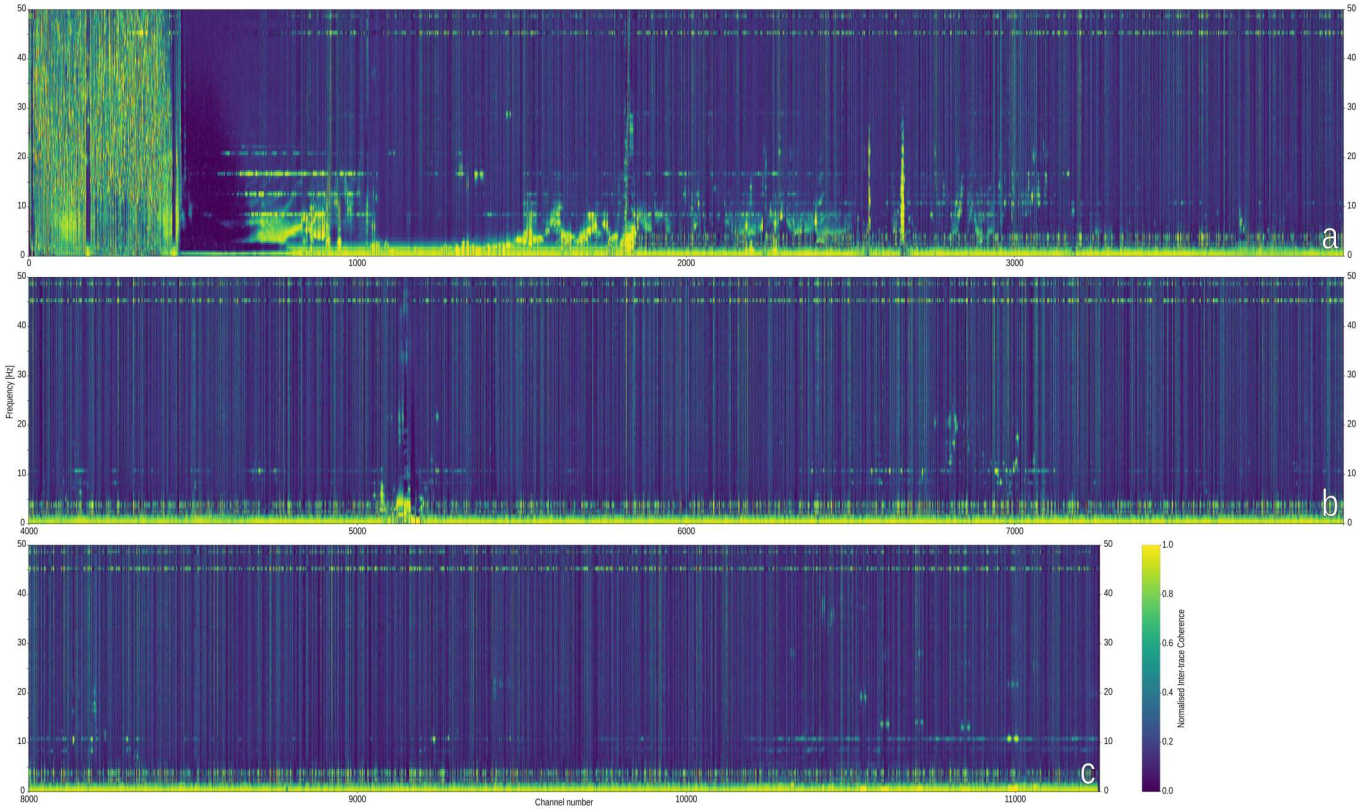

Figure S14 300 s frequency-channel coherence matrix of neighbouring channel pairs between 0 Hz and 50 Hz for all channels of the dataset on a 300 s window starting at 2023/10/28 15:30:00Z. a) channels 0-3999. b) channels 4000-7999. c) channels 8000-11293.

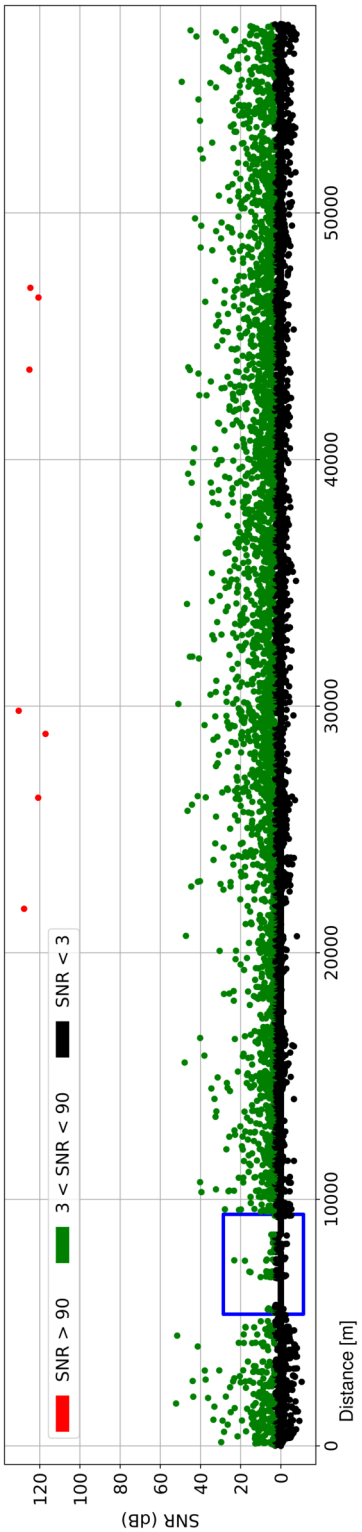

Figure S15 Signal-to-noise ratio sensitivity evaluation for each channel during a M2.7 local seismic event. Each dot corresponds to an individual channel. Colours represent sensitivity to the P wave arrival. Red: signal-to-noise ratio values above 90 dB, indicating consistent saturation. Green: signal-to-noise ratio between 3 dB and 90 dB, indicating good sensitivity. Black: lower sensitivity to this specific event. Blue rectangle highlights the area where the energy from the swell overpowers all other signals.

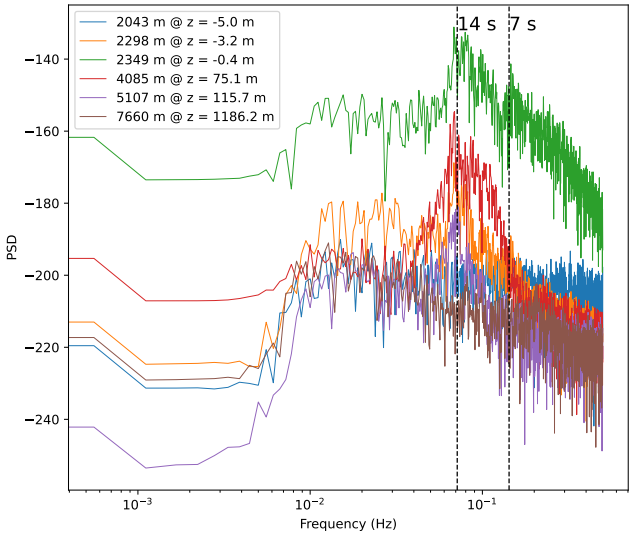

Figure S16 Median power spectral density of selected channels for a DAS recording over a 30-minute interval (start time: 2023/10/27 13:59:59Z), downsampled to 1 Hz and high-pass filtered with a corner frequency of 0.01 Hz.

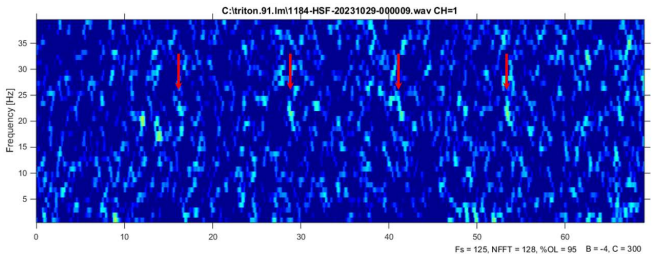

Figure S17 Spectrogram for Figure 16b. $NFFT = 128$, overlap 95 %. Red arrows indicate the whale calls.

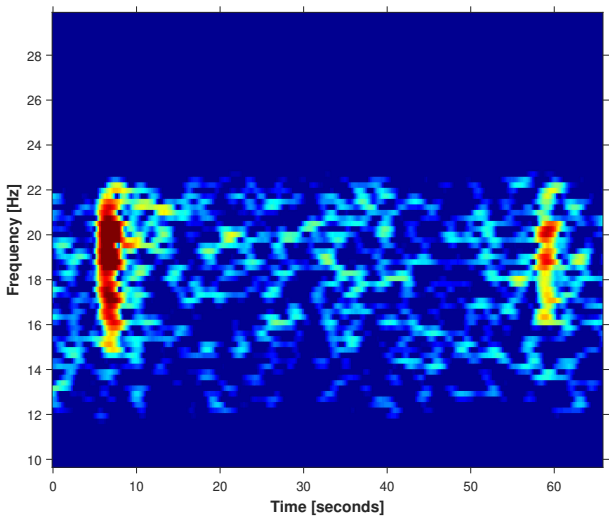

Figure S18 Spectrogram for baleen whale signal. 70 s spectrogram of data from a single channel at $\sim$20.01 km for the large amplitude signal identified in Figure 16a. $NFFT = 512$, overlap 95 %. To highlight the signal, data was filtered with an 8th order bandpass Butterworth filter between 12 Hz and 22 Hz.

References

Crotwell, H. P., Owens, T. J., and Ritsema, J. The TauP Toolkit: Flexible Seismic Travel-time and Ray-path Utilities. *Seismological Research Letters*, 70(2):154–160, March 1999. doi: 10.1785/gssrl.70.2.154.

Kennett, B. L. N. and Engdahl, E. R. Traveltimes for global earthquake location and phase identification. *Geophysical Journal International*, 105(2):429–465, May 1991. doi: 10.1111/j.1365-246x.1991.tb06724.x.